Study of the physiological parameters of a regulated oxygen mask

Geoffray Battiston, Dominique Beauvois, Gilles Duc, Emmanuel Godoy

HAL Id: hal-02963604
https://hal.science/hal-02963604v2

Submitted on 7 Dec 2022

Study of the physiological parameters of a regulated oxygen mask (updated version)

Geoffray Battiston[1], Dominique Beauvois[1] Gilles Duc, and Emmanuel Godoy[1]

Laboratoire des Signaux et Systèmes (L2S), Centrale-Supélec, CNRS, Université Paris-Sud, Université Paris-Saclay, 3 rue Joliot Curie, 91192 Gif sur Yvette cedex, France

Abstract. This paper is an extension to a previous work concerning the study of a regulated oxygen mask which distributes oxygen in response to an inhalation demand and shows a vibratory behaviour after a certain constant flow demand value. It was shown that it was a chattering effect due to the appearance of an unstability of the model equilibrium trajectory. After a brief summary of the previous results, a focus is made on the physiological parameters of the regulated mask which limit any modification of the mask.

Keywords: stability analysis, pneumatic systems

1 Introduction

The regulated oxygen mask is a purely mechanical device which distributes oxygen in response to an inhalation demand. During an inhalation, the mask volume is depleted, its pressure decreases and an oxygen distribution circuit is activated to compensate this demand. Over a certain demand flow value, the system starts chattering.

There is a classical methodology for studying pneumatic chattering systems. It consists of performing a linear stability analysis to infer the stability of the system equilibrium trajectories and a nonlinear stability analysis (with the use of normal form reductions, center manifold reductions and Lyapunov exponents) to study the trajectories of the system before a collision happens. This event is called a grazing bifurcation. Examples for classical pneumatic components like pressure-relief valves can be found in [1][2][3][4].

In [5], only the linear stability analysis was performed. First, a physical model for the regulated oxygen mask was proposed. Then, the equilibria of this nonlinear model were found. Since the mask vibratory behaviour appears after a certain demand flow value, it was chosen to analyse the evolution of the eigenvalues of the linearized varying model to check if some of them were positive after this threshold. It was indeed the case. Simulation showed a valve diverging and striking its seat, which is the chattering effect. The application of the Routh criterion allowed to find inequalities on physical parameters to ensure the stability of the regulated oxygen mask. Among various strategies, it appeared

that the increase of the value of a spring stiffness was sufficient to satisfy the Routh criterion. This increase was tested experimentally and it appeared that the trajectory of the regulator was sufficiently stabilized to avoid the chattering. Consequences of this increase like the decrease in the mask pressure, the increase of the amplitude of transient oscillations were observed and partly explained.

One conclusion of the previous work showed the improvement of the mask had to be made with attention to the respect of the physiological confort of the inhalating person. In this paper, we start by quoting the useful results from [5] in section 2, and study this confort matter in section 3, by analysing the important physiological parameters of the mask. The principles of an optimisation programming to improve the stability of the mask and its physiological performances are quickly presented in section 4.

2   Conclusions from previous work

This section quickly summarizes the results from [5]. It first focuses on the physical model of the mask in subsection 2.1. Then, it deals with the equilibrium trajectory of the mask in subsection 2.2 and the Routh conditions to have it stable in subsection 2.3.
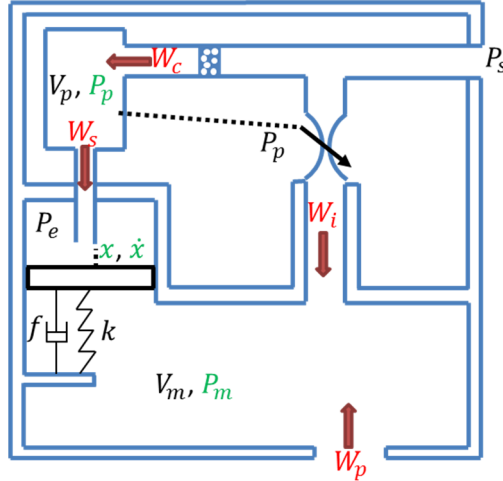
2.1   Physical model of the mask

Fig. 1: Definition sketch of the mathematical model (taken from [5]). Mass flows are drawn in red, the future state variables are written in green. The dashed line represents a pressure measurement.

Fig.1 represents a simplified diagram of the regulated oxygen mask to construct its mathematical model. The oxygen suppy is made at the opening with pressure P_s. The flow demand from the inhalating person is W_p. The flow distributed by

the mask is W_i. The pressure in the mask is P_m. The mass conservation in the mask volume V_m is:

$$\dot{P}_m = \frac{rT}{V_m}(W_i + W_p) \qquad (1)$$

where T is the temperature of the oxygen, which is considered constant in every subsequent volume, and r is the oxygen gas constant (for simplicity, it is supposed that there is only oxygen in the mask volume, which is not true in practice because of the exhalation of carbon dioxide from the equipped person).

The comparator is a rigid disk of section S_m, mass m, tied to a k-stiffness spring and a viscous damper f. It can close a tube of internal section S_s from which oxygen can evacuate. The distance between the orifice of this tube and the comparator is x, and equals zero when the tube is closed. $\dot{x}$ is the comparator speed. Exterior pressure P_e and pressure P_m apply on the surface S_m. On surface S_s are applied pressure P_p and pressure P_m. It can be shown (see [5] for the details) that the equation of the comparator can be written as:

$$m\ddot{x} + f\dot{x} + kx = S_m(P_e - P_m - dP_0) + S_s(P_p - P_s) \qquad (2)$$

where dP_0 is the comparator opening threshold. Its role will be studied later.

The evolution of the pilot chamber pressure P_p depends on the mass conservation equation:

$$\dot{P}_p = \frac{rT}{V_p}(W_c - W_s) \qquad (3)$$

where V_p is the pilot chamber volume.

W_s is the mass flow exiting this chamber through the comparator orifice:

$$W_s = k_s x P_p \qquad (4)$$

where k_s is the tube flow constant for a critical compressible flow.

W_c is the mass flow going through an isothermal Hagen-Poiseuille restriction of coefficient k_c:

$$W_c = k_c(P_s^2 - P_p^2) \qquad (5)$$

The regulating actuator takes a measurement of P_p and sends a mass flow W_i proportionnal to it:

$$W_i = \begin{cases} k_i(P_s - P_t - P_p) \, , & P_p \leq P_s - P_t \\ 0 & , \; P_p > P_s - P_t \end{cases} \qquad (6)$$

where P_t is the threshold for $P_s - P_p$ to start delivering a mass flow.

2.2   Equilibrium trajectory of the mask

We use equations (1-6) to write the state equations:

$$\dot{X} = \begin{bmatrix} \dot{x} \\ -\frac{k}{m}x - \frac{f}{m}\dot{x} - \frac{S_m}{m}P_m + \frac{S_s}{m}P_p + H \\ -k_i\frac{rT}{V_m}P_p + \frac{rT}{V_m}W_p + \frac{rT}{V_m}k_i(P_s - P_t) \\ \frac{rT}{V_p}(-k_cP_p^2 - k_sxP_p) + \frac{rT}{V_p}k_cP_s^2 \end{bmatrix} \qquad (7)$$

in which the state vector is defined by:

$$X = \begin{bmatrix} x \\ \dot{x} \\ P_m \\ P_p \end{bmatrix} \tag{8}$$

and H is given by:

$$S_m(P_e - dP_0)/m - S_s P_s/m \tag{9}$$

Equilibrium state variables are written with a bar:

$$\bar{P}_m = \left(S_m(P_e - dP_0) + S_s(\bar{P}_p - P_s) - k\bar{x} \right)/S_m \tag{10}$$
$$\bar{P}_p = W_p/k_i + P_s - P_t \tag{11}$$
$$\bar{x} = k_c/k_s(P_s^2/\bar{P}_p - \bar{P}_p) \tag{12}$$

It was shown in [5] that two eigenvalues of the 4-dimension evolution matrix of the model linearized around equilibrium state variables were having a positive real part value, which was coincident with the diverging position of the comparator. This one was then colliding with its seat. The time of the first strike was the same as the time of the beginning of chattering. An example is shown in Fig.2-4.
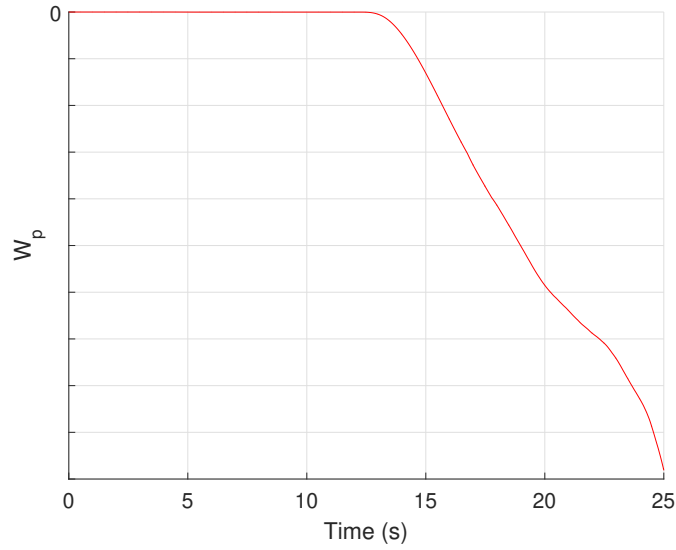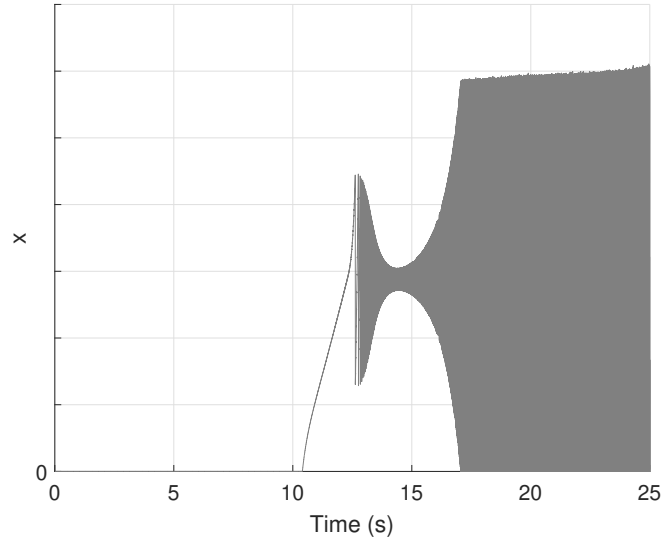

Fig. 2: W_p as a ramp demand.

Fig. 3: Opening x of the comparator vs time. Near 17s, it goes back to zero. This is the start of chattering.
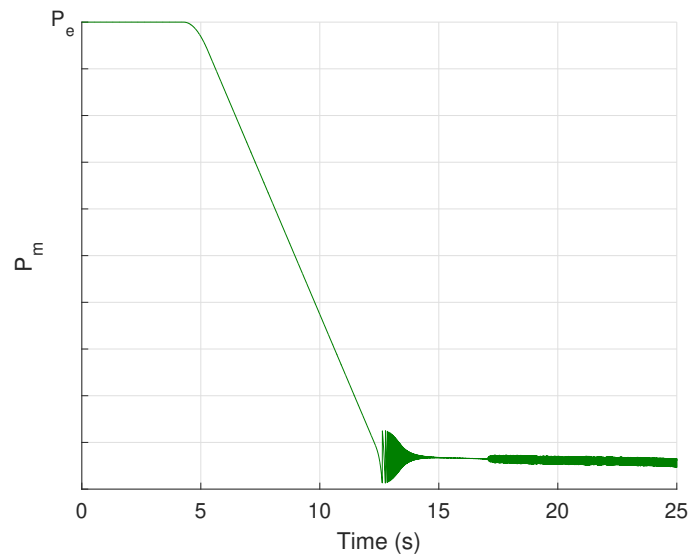

Fig. 4: Mask pressure P_m vs time. Near 17s, after a flat transition, it starts chattering.

2.3   Results from the appplication of the Routh criterion

After linearizing the state equations around the equilibrium trajectory and considering the characteristic polynomial of the obtained evolution matrix, it is possible to apply the Routh criterion to find inequalities on the physical parameters to make the mask stable during an inhalation. The first inequality was:

$$\frac{kf}{m^2} - \frac{rTk_sS_s}{V_pm}\bar{P}_p > 0 \tag{13}$$

The second inequality was obtained after some complementary assumptions which will not be described here:

$$\frac{rTk_iS_m}{V_pm^2}\left(\frac{f}{m} + \frac{10rTk_cP_s}{3V_p}\right)^2 < R \tag{14}$$

with:

$$R = \left(\frac{rTP_s(4k_c + k_sS_p)}{V_pm}\right)^2 +$$
$$\left(\frac{rTP_s(2k_c + k_sS_p)}{V_pm}\right).\left(\frac{k}{m} + \frac{rTf}{V_pm}k_c2P_s\right).\left(\frac{f}{m} + \frac{rT}{V_p}k_c2P_s\right) \tag{15}$$

A sufficient condition to ensure these inequalities was to increase the spring stiffness k. This suggestion was tested experimentally, and made the mask stable in simulations and less vibrating in experiments, at the cost of degraded physiological performances [5].

3   Study of the mask physiological parameters

Paper [5] was more focused on the linear stability analysis of the regulated oxygen mask. Presently, we will study the mask physiological parameters, a short name to call physical quantities of the mask which have a physiological influence on a breathing person. There are 4 in total: the opening time t_{op} (section 3.1), the closing time t_{cl} (section 3.2), the equilibrium mask pressure values $\bar{P_m}$ (section 3.3), the mask pressure overshoot P_m^* in response to a step-demand (section 3.4). Some of them cannot be derived analitically, so we will sometimes have resort to numerical approximations.

3.1   Opening time

The opening time t_{op} is defined as the time between the beginning of an inhalation and the beginning of the oxygen distribution. It must not be too large for the inhalating person to receive oxygen as soon as possible. This value is difficult to obtain analytically. It is estimated through some assumptions which will be presented later.

At $t = 0$, $P_m = P_e$, and for the very beginning of an inhalation, the demand is approximated with a ramp function:

$$W_p = -wt \tag{16}$$

with w the positive slope coefficient of the ramp. The comparator is closed as long as $P_m > P_e - dP_0$. The only working equation is (1). Its solution is:

$$P_m(t) = P_e - \frac{wrT}{2V_m}t^2 \tag{17}$$

The comparator opens at time t_{co}:

$$t_{co} = \sqrt{\frac{2V_m dP_0}{wrT}} \tag{18}$$

The next time that is needed is the time t_{ac} between the opening of the comparator and the one of the actuator activation. It is needed to solve (2) and (3) at the same time, which is difficult and may lead to a transcandental equation in t_{ac}. Simulations of P_m, x and P_p are shown in Fig.5-7.
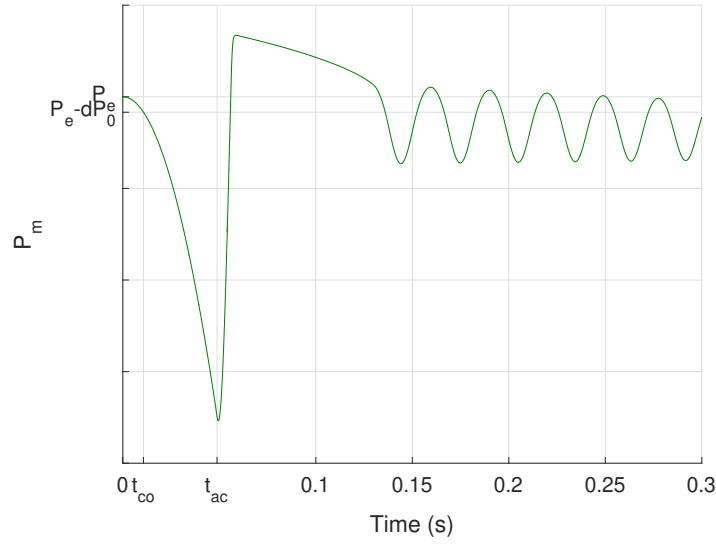

Fig. 5: P_m at the beginning of a ramp demand. At t_{co}, $P_m = P_e - dP_0$.

It can be observed in Fig.8 that for the actual mask parameter settings, the dynamics of the comparator can be neglected. Then, equation (2) can be simplified:

$$x = \frac{S_m}{k}(P_e - dP_0 - P_m) + \frac{S_s}{k}(P_p - P_s) \tag{19}$$

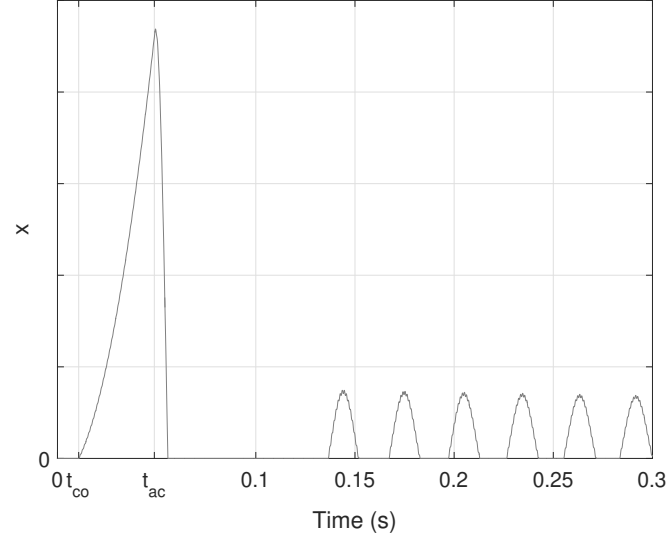$$\dot{P}_p = \frac{rT}{V_p}(k_c(P_s^2 - P_p^2) - k_s x P_p) \tag{20}$$

Fig. 6: x at the beginning of a ramp demand. At t_{co}, the comparator opens.

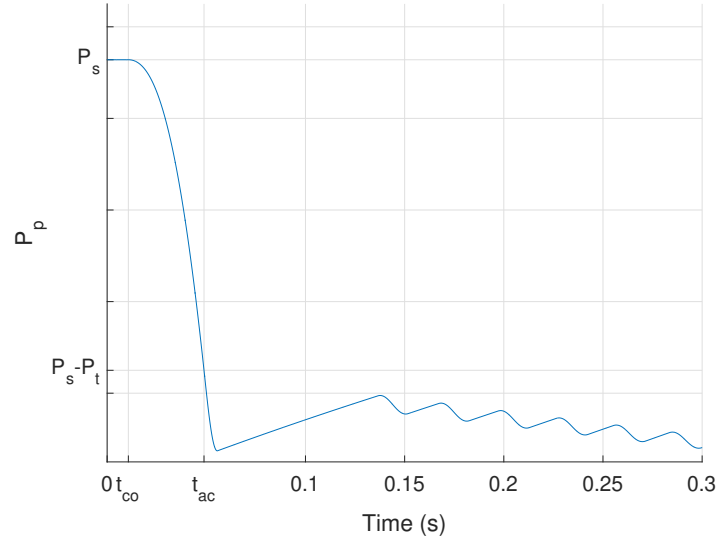

Fig. 7: P_p at the beginning of a ramp demand. At t_{co}, the pressure starts decreasing and at t_{ac} it reaches $P_s - P_t$ which is the time at which the actuator is activated.
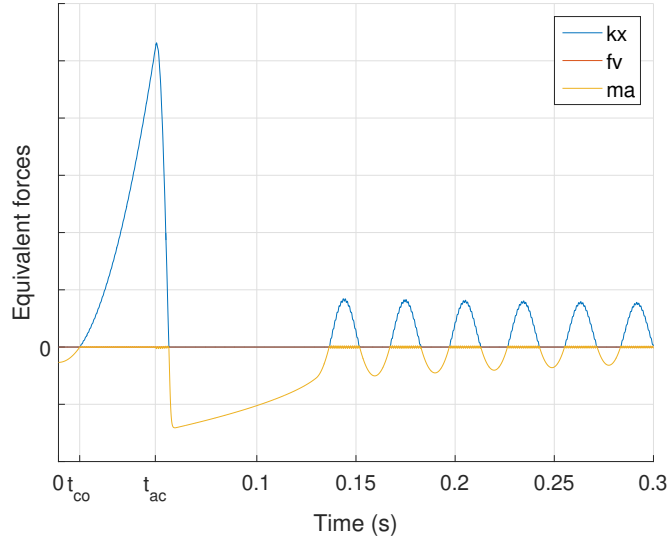
Fig. 8: Comparison between kx, $fv = f\dot{x}$ and $ma = m\ddot{x}$ at the beginning of a ramp demand.

Since the actuator is still not sending oxygen, equation (17) is used in (19), yielding to:

$$\dot{P}_p = \frac{rT}{V_p}\left(k_c(P_s^2 - P_p^2) - k_s P_p\Big(\frac{S_m}{k}\big(\frac{wrT}{V_m}t^2 - dP_0\big) + \frac{S_s}{k}(P_p - P_s)\big)\right) \quad (21)$$

We change the time origin by writting $t = t' + t_{co}$. The mask pressure can be rewritten:

$$P_m = P_e - \frac{wrT}{2V_m}(t' + t_{co})^2 \quad (22)$$

This is reinserted in (21):

$$\dot{P}_p = \frac{rT}{V_p}\left(k_c(P_s^2 - P_p^2) - k_s P_p\Big(\frac{S_m}{k}\big(\frac{wrT}{V_m}(t' + t_{co})^2 - dP_0\big) + \frac{S_s}{k}(P_p - P_s)\big)\right) \quad (23)$$

Which we write for simplicity:

$$\dot{P}_p \simeq -bP_p^2 + cP_p + d - e(t' + t_{co})^2 \quad (24)$$

with $b = \frac{rT}{V_p}(k_c + \frac{k_s S_s}{k})$, $c = \frac{rTk_s}{kV_p}(S_m dP_0 + S_s P_s)$, $d = \frac{rT}{V_p}k_c P_s^2$, $e = -\frac{rT}{V_p}\frac{k_s P_s S_m}{k}\frac{wrT}{2V_m}(t'+t_{co})^2$ and where in e the factor P_p has been approximated with P_s. This approximation is linked to the fact that in practice $P_s - P_p < 0.1P_s$.

Solving this Riccati equation is very difficult. This difficulty can be overcome with numerical approximations. The pilot pressure P_p will be visible on Fig.9.

P_p seems to be quadratic from t_{co}. We want P_p to approximate the following time equation:

$$P_p = P_s - at'^2 \qquad (25)$$

This approximation is inserted in the differential equation (24).

$$-2at' \simeq -bP_s^2 + cP_s + d - et_{co}^2 - 2et_{co}t' + (2bP_sa - ca - e)t'^2 \qquad (26)$$

where t'^4 has been neglected. After a short calculus, it can be shown that the constant term $-bP_s^2 + cP_s + d - et_{co}^2$ is equal to 0. a is a constant, so we need to get rid of t' from $a = (2et_{co} + et')/((2bP_s - c)t' + 2)$. In the first case (low t'):

$$a_1 = et_{co} \qquad (27)$$

In the second one (high t'):

$$a_2 = \frac{e}{2bP_s - c} \qquad (28)$$

These two approximations of P_p are plotted in Fig.9. It appears the first approximation is better that the second one.
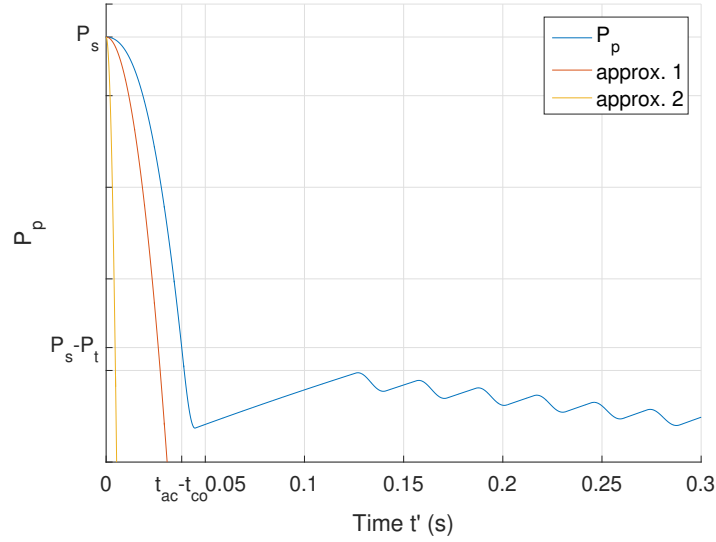

Fig. 9: Comparison of P_p and its two approximations 1 and 2 with respective coefficients a_1 and a_2.

From there, we seek for the time t_{ac} at which the actuator opens, that is when $P_p = P_s - P_t$:

$$P_s - P_t = P_s - a_1 t_{ac}^2 \qquad (29)$$

which gives:

$$t_{ac} = \sqrt{\frac{P_t}{a_1}} \tag{30}$$

ie:

$$t_{ac} = \sqrt{\frac{kP_t V_p \sqrt{2V_m}}{k_s S_m P_s rT \sqrt{rTwdP_0}}} \tag{31}$$

It appears that t_{ac} doesn't take into account S_s and k_c. In fact, it can be checked that their influence is indeed not very remarkable during the fall of P_p, see Fig.10. Simulation also shows that multiplying or dividing S_s by 5 leaves P_p almost
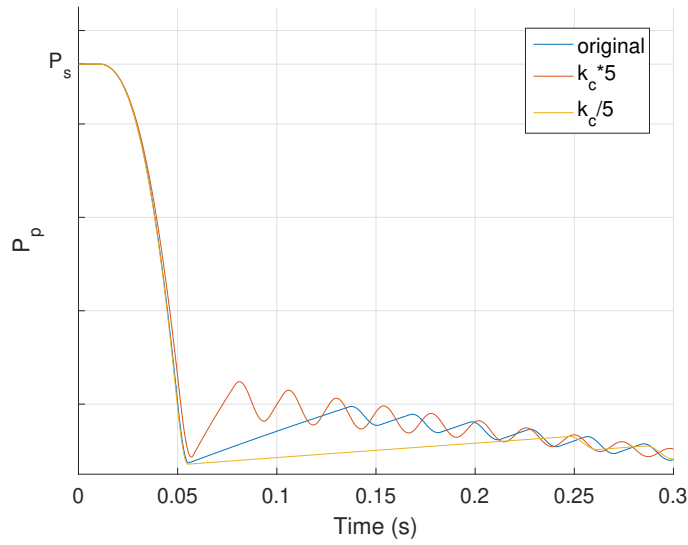

Fig. 10: Fall of P_p for different k_c.

unchanged. In order to be able to use t_{ac} for an eventual optimisation of the mask parameters, we use a rule of thumb by rewritting it:

$$t_{ac} = \alpha \sqrt{\frac{kP_t V_p \sqrt{2V_m}}{k_s S_m P_s rT \sqrt{rTwdP_0}}} \tag{32}$$

where α is a correcting factor to make correspond the real t_{ac} and the approximated one in the case of the original parameter settings. This incidently supposes that the variations of the real t_{ac} are followed by its approximating formula.

Deduction of the opening time: The opening time can finally be written:

$$t_{op} = t_{co} + t_{ac} \tag{33}$$

In order to decrease t_{co}, one can decrease V_m and dP_0. To decrease t_{ac}, one can decrease k and P_t for instance, and increase dP_0 and S_m.

3.2 Closing time

The closing time t_{cl} is the duration between the closing of the comparator and the end of oxygen distribution. If it is too high, oxygen still flows after the end of an inhalation and the beginning of the exhalation, which is disturbing for one who breathes in the mask. If the comparator closes its seat, the working equations for the mask are:

$$\dot{P}_p = \frac{rT}{V_p} W_c = \frac{rTk_c}{V_p}(P_s^2 - P_p^2) \tag{34}$$

The analytical solution of this differential equation exists. It can be found using the separation of variables:

$$2P_s\frac{rTk_c}{V_p}dt = \frac{2P_s dP_p}{(P_s - P_p)(P_s + P_p)} = \frac{dP_p}{P_s - P_p} + \frac{dP_p}{P_s + P_p} \tag{35}$$

This equation is then integrated between $t = 0$ and t, P_{p0} and P_p:

$$P_p = P_s \frac{\exp\left(2P_s \frac{rTk_c}{V_p}t\right) - \frac{P_s - P_{p0}}{P_s + P_{p0}}}{\exp\left(2P_s \frac{rTk_c}{V_p}t\right) + \frac{P_s - P_{p0}}{P_s + P_{p0}}} \tag{36}$$

for a starting pilot pressure $P_p(t = 0) = P_{p0}$. The mask stop sending oxygen at the moment the actuator is desactivated, that is to say for $P_p = P_s - P_t$. We write $t_{cl} = \{t, P_p(t) = P_s - P_t\}$, the closing time. Solving (36) for t_{cl} yields:

$$t_{cl} = \frac{V_p}{2P_s rTk_c} \ln\left(\frac{2P_s - P_t}{P_s + P_{p0}} \frac{P_s - P_{p0}}{P_t}\right) \tag{37}$$

The closing time increases with V_p and P_t and decreases with k_c. However, one must not conclude that making k_c very large is a good idea: if the restriction is small, the opening of the comparator may not be sufficient enough to empty the pilot volume and then send oxygen: someone inhalating could suffocate. A compromise shall be found.

3.3 Mask pressure value

For the mask to be easy to breathe in, the equilibrium mask pressure $\bar{P}_m$, needs to be as high as possible (high pressure gas flow more easily in lower pressure areas such as the lungs during inhalation). Using (10), (11) and (12), the expression of $\bar{P}_m$ is:

$$\bar{P}_m = (P_e - dP_0) + \frac{S_s}{S_m}\left(\frac{W_p}{k_i} - P_t\right) - \frac{kk_c}{k_s S_m}\left(\frac{P_s^2}{\frac{W_p}{k_i} + P_s - P_t} - (\frac{W_p}{k_i} + P_s - P_t)\right) \tag{38}$$

It obviously depends of the demand flow W_p. The derivative along W_p is:

$$\frac{\partial \bar{P}_m}{\partial W_p} = \frac{S_s}{S_m k_i} + \frac{k k_c}{k_s S_m} \left(\frac{P_s^2}{k_i \left(\frac{W_p}{k_i} + P_s - P_t \right)^2} + \frac{1}{k_i} \right) \tag{39}$$

It is always positive. Nevertheless, one must remember that the convention for W_p is a flow entering the mask. Then, it is negative for an inhalation, which also means that $\bar{P}_m$ decreases with the increase of the demand. If $\bar{P}_m$ must not decrease too much with W_p, one can decrease as much as possible this derivative, that is to say increase k_i, S_m, or decrease S_s, k or k_c.

3.4   Mask pressure overshoot

The last physiological parameter is the mask pressure overshoot P_m^*. In this case, the demand is not set as a ramp, but a step $W_{p,0}$. In Fig.11, we plot W_i and $-W_p$ to see at which moment they cross each other, and observe this time t^* coincides with the one at which P_m reaches its overshoot.
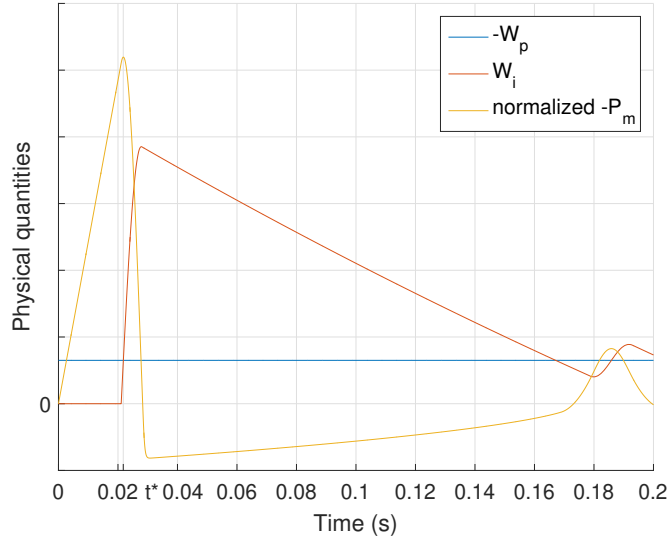

Fig. 11: Plot of normalized P_m and W_i in response to a step demand $-W_p$. t^* is more on the left that it appears.

In fact, P_m reaches its overshoot value P_m^* when $\dot{P}_m = 0$, that is to say $W_i = -W_{p,0}$ (if the demand was not a ramp, we woud not know exactly at which flow value the derivative of P_m would be zero). According to (11), we can approximate:

$$P_p^* = P_s - P_t + \frac{W_{p,0}}{k_i} \tag{40}$$

At this point, the mask dynamics is (stars refer to the value at t^*):

$$\dot{P_p}^* = \frac{rT}{V_p}\big(k_c(P_s^2 - P_p^{*2}) - k_s x^* P_p^*\big) \tag{41}$$

$$m\ddot{x}^* + f\dot{x}^* + kx^* = S_m(P_e - dP_0 - P_m^*) + S_s\big(-P_t + \frac{W_{p,0}}{k_i}\big) \tag{42}$$

That is:

$$P_m^* = P_e - dP_0 + \frac{S_s}{S_m}\big(-P_t + \frac{W_{p,0}}{k_i}\big) - \frac{1}{S_m}(m\ddot{x}^* + f\dot{x}^* + kx^*) \tag{43}$$

In order to get P_m^*, the values of x^*, $\dot{x}^*$ and $\ddot{x}^*$ are needed. It seems difficult to get a sufficiently satisfactory analytical approximation for these derivatives. Nevertheless, the same approximation as (19) can be made. We finally get an approximation for the overshot P_m^*:

$$P_m^* = P_e - dP_0 + \frac{S_s}{S_m}(-P_t + \frac{W_{p,0}}{k_i}) - \frac{k}{k_s S_m P_p^*}(k_c(P_s^2 - P_p^2) - \frac{V_p \dot{P_p}^*}{rT}) \tag{44}$$

We suppose $|rTk_c(P_s^2 - P_p^2)| \ll |V_p \dot{P_p}^*|$, which comes from a simulation observation, see Fig.12.
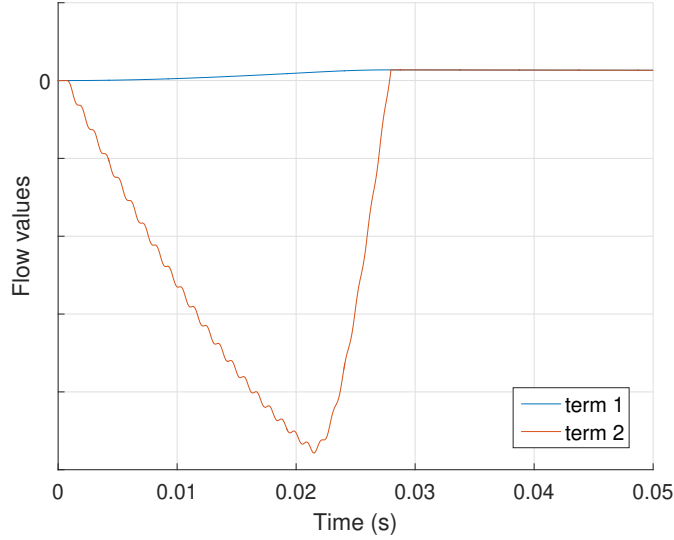

Fig. 12: Comparison between the first and second term of the last parenthesis of (44).

The last remaining problem is to get the value of $\dot{P_p}^*$. The same approximation as in (25) for P_p is made:

$$P_p = P_s - at'^2 \tag{45}$$

where $t' + t_1 = t$ and t_1 is the time at which the comparator opens. We give it another name than t_{co} to avoid confusion: these two times are not the same because the demand is a step and not a ramp anymore. This time, the coefficient a is directly set with the activation time t_{ac}:

$$P_p(t' = t_{ac}) = P_s - P_t = P_s - at_{ac}^2 \tag{46}$$

ie:

$$a = \frac{P_t}{t_{ac}^2} \tag{47}$$

The time at which $P_p = P_p^*$ is defined by (approx. 40):

$$P_s - at^{*2} = P_s - P_t + \frac{W_{p,0}}{k_i} \tag{48}$$

so:

$$t^* = \sqrt{\frac{1}{a}(P_t - \frac{W_{p,0}}{k_i})} \tag{49}$$

This gives the last wanted term as a better approximation:

$$\dot{P_p}^* = -2\frac{P_t}{t_{ac}^2}t^* \tag{50}$$

Equation (44) can finally be fully written:

$$P_m^* = P_e - dP_0 + \frac{S_s}{S_m}(-P_t + \frac{W_{p,0}}{k_i}) - 2\frac{k}{k_s S_m P_p^*}\frac{V_p}{rT}\frac{P_t}{t_{ac}}\sqrt{1 - \frac{W_{p,0}}{k_i P_t}} \tag{51}$$

Obviously, the time t_{ac} is not the same for a step demand flow as the one for a ramp demand flow. Nevertheless, it is possible to get an approximation of it in the same way as for the previous case. One would have to use (24) and replace t_{co} and e with their new values.

In order to decrease the overshoot, ie increase P_m^* (because P_m decreases with a inhalation and the overshoot is bottom-oriented), one must decrease dP_0, S_s, P_t, k or increase S_m, k_i, k_s. These tendencies were confirmed with multiple simulations for different parameter settings.

4   Improvement of the mask behaviour

As a summary of this work, in order to improve the mask behaviour, it is needed to satisfy conditions (13) and (14) while decreasing the opening time (33), the closing time (37), the mask pressure overshoot (51) and increasing the equilibrium mask pressure (38). As it was already stated in a different way, modifying one parameter may not be sufficient and it is needed to solve an optimisation problem.

This matter was not yet tackled with. Nevertheless, it is possible to precise how it is going to be dealt with. Obviously, one point will concern the choose

of the cost function which will at least take into the physiological parameters. Another element must be taken into consideration even if it is not obvious: the cost function must also integrate the size of the region of stability around the position of the minimum. As a matter of fact, the physical values of the mask components are not mastered with full accuracy. If the stability-physiologically optimized region is narrow, we may end up with leaving it easily due to experimental settings inaccuracy. There also are uncertainties in the model (one about S_s was explained in [5]). We may find a less physiologically performant region but with more room for parameters settings. At last, one point concerns the geometry limitations for the mask which must be added as additional constraints to the stability conditions.

5   Conclusion

The stability analysis of the studied regulated oxygen mask performed in [5] gave stability regions which needed to be refined to take into account physiological performance. The physiological parameters of the mask were given thanks to multiple assumptions in this paper. Future works will be devoted to an optimisation programming in order to find parameters configurations for which both performance and stability are reached.

References

1. MacLeod, G (1985) Safety valve dynamic instability: an analysis of chatter. J. Pressure Vessel Technol 107(2), pp 172-177 .
2. Maeda, T (1970) Studies on the dynamic characteristic of a poppet valve: 1st report, theoretical analysis. Bulletin of JSME, 13(56), pp 281-289.
3. Hayashi, S, Hayase, T, Kurahashi, T (1997) Chaos in a hydraulic control valve. Journal of fluids and structures, 11(6), pp 693-716.
4. Licsko, G, Champneys, A, Hos, C (2009) Nonlinear Analysis of a Single Stage Pressure Relief Valve. International journal of applied mathematics, 39(4).
5. Battiston, G, Beauvois, D, Duc, G, Godoy, E (2018) Stability analysis of a regulated oxygen mask. Proceedings of the 15th International Conference on Informatics in Control, Automation and Robotics - Volume 1: ICINCO (2018). doi:10.5220/0006848203270334